Landau-Quantized Excitonic Absorption and Luminescence in a Monolayer Valley Semiconductor

Erfu Liu,[1] Jeremiah van Baren,[1] Takashi Taniguchi,[2] Kenji Watanabe,[2] Yia-Chung Chang,[3] and Chun Hung Lui[1,*]
[1]Department of Physics and Astronomy, University of California, Riverside, California 92521, USA
[2]National Institute for Materials Science, Tsukuba, Ibaraki 305-004, Japan
[3]Research Center for Applied Sciences, Academia Sinica, Taipei 11529, Taiwan

(Received 16 August 2019; revised manuscript received 9 October 2019; accepted 17 January 2020; published 3 March 2020)

We investigate Landau-quantized excitonic absorption and luminescence of monolayer WSe_2 under magnetic field. We observe gate-dependent quantum oscillations in the bright exciton and trions (or exciton polarons) as well as the dark trions and their phonon replicas. Our results reveal spin- and valley-polarized Landau levels (LLs) with filling factors $n = +0, +1$ in the bottom conduction band and $n = -0$ to -6 in the top valence band, including the Berry-curvature-induced $n = \pm 0$ LLs of massive Dirac fermions. The LL filling produces periodic plateaus in the exciton energy shift accompanied by sharp oscillations in the exciton absorption width and magnitude. This peculiar exciton behavior can be simulated by semiempirical calculations. The experimentally deduced g factors of the conduction band ($g \sim 2.5$) and valence band ($g \sim 15$) exceed those predicted in a single-particle model ($g = 1.5$, 5.5, respectively). Such g-factor enhancement implies strong many-body interactions in gated monolayer WSe_2. The complex interplay between Landau quantization, excitonic effects, and many-body interactions makes monolayer WSe_2 a promising platform to explore novel correlated quantum phenomena.

DOI: 10.1103/PhysRevLett.124.097401

Monolayer transition metal dichalcogenides (TMDs, e.g., MoS_2 and WSe_2) host tightly bound excitons in two time-reversal valleys (K, K') with opposite spins, magnetic moment, Berry curvature, and circular dichroism [1–14]. With the application of magnetic field, the two valleys exhibit opposite Zeeman shift [15–19] and contrasting Landau levels (LLs) [20–22], including two LLs with filling factor $n = 0$ due to the Berry curvature of massive Dirac fermions [22–24] [Fig. 1(a)]. These two LLs are most relevant to the fractional quantum Hall effect and Wigner crystallization, which should first occur near the lowest LLs [25–28]. Besides, low-lying LLs contribute to the exciton formation. Given the small LL spacing (~10 meV) in TMDs due to the large carrier mass, an exciton with binding energy >150 meV is the superposition of many LLs. These distinctive features make monolayer TMDs an excellent system to explore novel exciton-LL coupling and many-body interactions in two dimensions.

Much interesting LL physics in TMDs has been revealed by transport, scanning probe, optical and single-electron-transistor spectroscopy [29–39]. But these experiments are subject to different limitations. For instance, high contact resistance and poor TMD material quality have limited transport probes to LLs with $n \geq 3$ in few-layer TMDs and $n \geq 17$ in monolayer TMDs [29–37]. Nonoptical probes cannot assess the excitonic states. Recent optical experiments reported inter-LL optical transitions in monolayer WSe_2, but only in the high-charge-density regime where the excitonic effect is much reduced [38]. Smolenski *et al.* recently reported excitonic quantum oscillations in monolayer $MoSe_2$, but only for absorption and $n \geq 1$ LLs of bright excitonic states [40]. More comprehensive studies are needed to explore the Landau-quantized excitonic physics for bright and dark excitonic states, with optical absorption and emission, on the electron and hole sides, and in a broad LL spectrum including the $n = 0$ LLs.

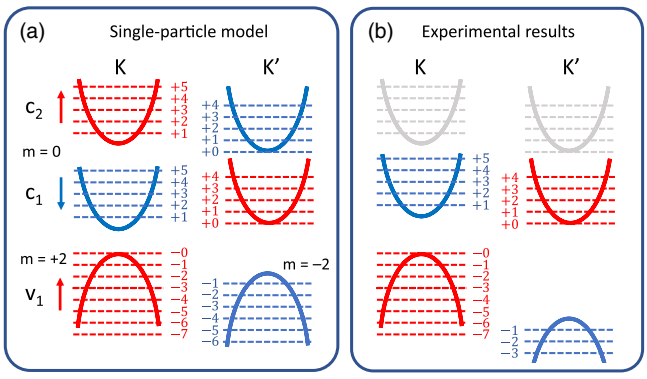

FIG. 1. (a) Schematic Landau levels (dashed lines) in monolayer WSe_2 predicted by a single-particle model. The arrows and color denote the electron spin in the conduction bands (c_1, c_2) and valence band (v_1). $m = 0$, ± 2 are the azimuthal quantum numbers of the atomic orbits in the conduction bands and valence band, respectively. (b) LLs revealed by our experiment, indicating strong enhancement of valley Zeeman shift by many-body interactions.

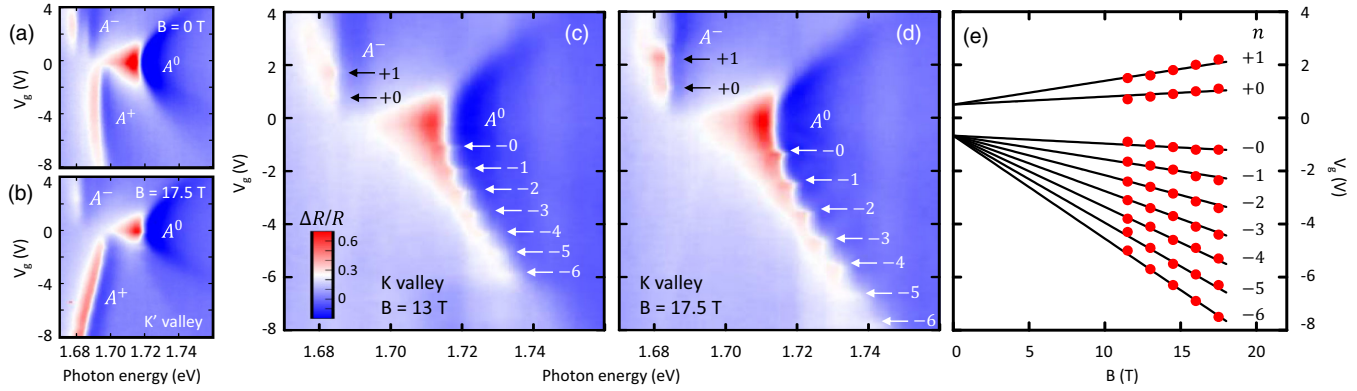

FIG. 2. (a) Gate-dependent $\Delta R/R$ reflectance contrast map of monolayer WSe_2 with no magnetic field. (b)–(d) Reflectance contrast maps in left-handed (b) and right-handed (c)–(d) circular polarization, corresponding to optical transitions in the K' and K valley, respectively, at magnetic fields $B = 13.0$ T (c) and $B = 17.5$ T (b),(d). The arrows denote the quantum oscillations. (e) The measured gate voltages (V_g) at half-filled LLs as a function of magnetic field. The lines are the fitted Landau fan diagram. n is the LL filling factor. Our fits show a $\Delta V_g \sim 1.2$ V gap between the electron and hole sides at $B = 0$ T, presumably due to the filling of defect states inside the band gap. The experiments were conducted at $T \sim 4$ K.

In this Letter, we investigate Landau-quantized excitonic absorption and luminescence in monolayer WSe_2 under magnetic fields up to $B = 17.5$ T. We observe gate-dependent quantum oscillations in the bright exciton and trions as well as the dark trions and their phonon replicas (here trions refer broadly to correlated states between excitons and the Fermi sea, including exciton polarons [41–43]). Our results reveal spin- and valley-polarized LLs with $n = -6$ to $+1$ from the hole to electron sides, including the two valley-contrasting $n = 0$ LLs [Fig. 1(b)]. The gate-dependent exciton energy shift exhibits periodic plateaus, accompanied by sharp oscillations in the exciton absorption width and magnitude. Such unusual exciton behavior can be simulated by semiempirical calculations. The g factors of the conduction and valence bands ($g \sim 2.5$, 15 respectively) exceed the predicted values in a single-particle model ($g = 1.5$, 5.5 respectively), implying strong many-body interactions in the system. Our research reveals complex interplay between Landau quantization, excitonic effects, and many-body interactions in monolayer WSe_2.

We investigate ultraclean monolayer WSe_2 gating devices encapsulated by hexagonal boron nitride on Si/SiO_2 substrates [44–47]. All the experiments were conducted at temperature $T \sim 4$ K. To study the absorption properties, we measure the reflectance contrast $\Delta R/R = (R_s - R_r)/R_r$, where R_s is the reflection spectrum on the sample position and R_r is the reference reflection spectrum on a nearby area without WSe_2. We selectively probe the optical transitions in the K and K' valleys with right- and left-handed circular polarization, respectively [11–14]. At zero magnetic field, the two valleys, being energy degenerate, exhibit the same gate-dependent $\Delta R/R$ map featuring the A exciton (A^0) and A trions (A^-, A^+) [Fig. 2(a)]. At strong out-of-plane magnetic fields up to $B = 17.5$ T, however, the K and K' valleys exhibit distinct $\Delta R/R$ response. While the K'-valley map is qualitatively similar to that at zero magnetic field [Fig. 2(b)], the K-valley map exhibits several differences [Figs. 2(c)–2(d)]. First, the A^+ trion is quenched. This is because the K valley lies higher than the K' valley under the magnetic field; the injected holes only fill the K valley [Fig. 1(a)]. The Pauli exclusion principle forbids the formation of A^+ trion with two holes in the K valley. Second, with the suppression of the A^+ trion, the K-valley A^0 exciton is retained on the hole side, where it exhibits pronounced oscillations with increasing hole density. Third, the A^- trion $\Delta R/R$ response also oscillates as the electron density increases. Fourth, the period of these oscillations increases linearly with the magnetic field [Figs. 2(c)–2(e)]. These results mimic the Shubnikov–de Haas oscillations in quantum transport and strongly suggest the formation of LLs [29–39].

From the reflectance contrast maps, we extract the real part of the optical sheet conductivity (σ) of monolayer WSe_2 by solving the optical problem in our device structure (see Supplemental Material [47]). σ is proportional to the optical absorption of monolayer WSe_2. Figure 3(a) displays the σ map of the K-valley A^0 exciton at $B = 17.5$ T. Figures 3(b)–3(d) show the extracted exciton peak energy, peak width, peak conductivity, and integrated conductivity as a function of gate voltage (V_g). Remarkably, periodic plateaus appear as the exciton energy blueshifts on the hole side. At the step edges, the exciton peak is maximally broadened, and the peak conductivity drops to a local minimum. But the integrated conductivity drops relatively smoothly with V_g.

These quantized and oscillatory excitonic features can be qualitatively understood by the LL formation. At zero magnetic field, the hole injection gradually increases the screening and state-filling effects. This will renormalize the band gap and reduce the exciton binding energy, leading to

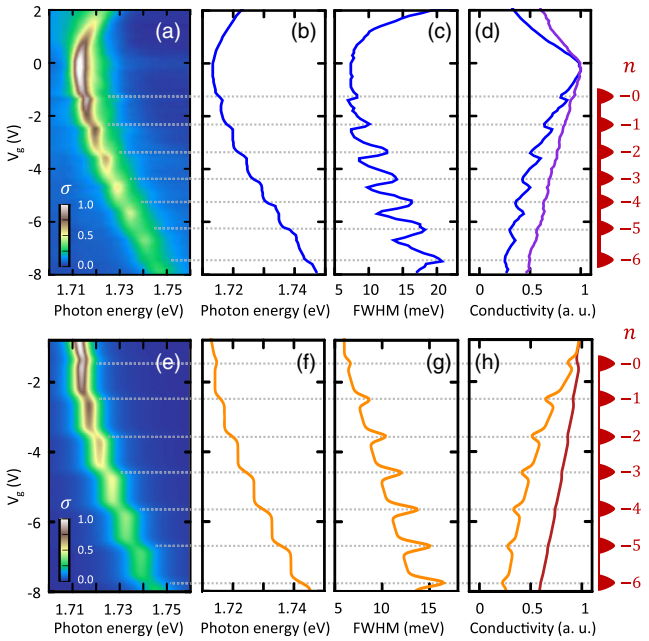

FIG. 3. (a) The optical sheet conductivity of A^0 exciton extracted from Fig. 2(d). (b) The exciton peak energy, (c) full width at half maximum (FWHM), (d) peak conductivity (blue) and integrated conductivity (purple), extracted from (a). (e) The theoretical exciton conductivity map, (f) peak energy, (g) FWHM, (h) peak conductivity (orange) and integrated conductivity (red). All conductivity values are normalized to 1. The dashed lines denote the half-filled LL positions.

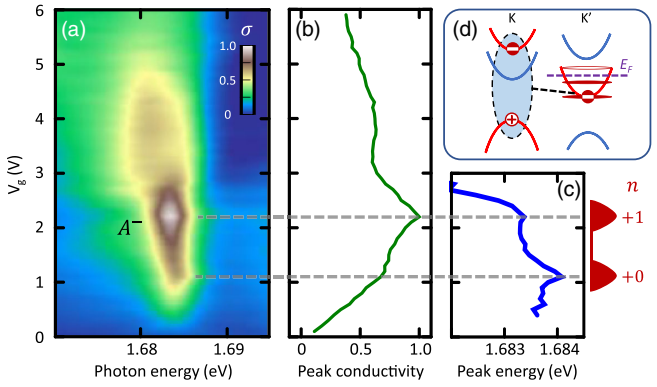

FIG. 4. (a) The normalized sheet conductivity of A^- trions extracted from Fig. 2(d). (b) The trion peak conductivity and (c) peak energy extracted from (a). The dashed lines denote the half-filled LL positions. (d) The schematic band configuration of intervalley A^- trion with the relevant LLs and Fermi energy (E_F).

a smooth blueshift of exciton resonance energy [42,43,77,78]. The smooth process will be disrupted when LLs are formed. When the Fermi energy (E_F) varies within a LL gap, the screening and state-filling effects remain unchanged; the exciton energy will not shift with V_g and hence a plateau appears; the LL gap will also suppress the carrier scattering and narrow the exciton peak. But when the Fermi energy varies within a LL with singular density of states, the rapid increase of hole density will drastically increase the screening and state-filling effects, leading to a steplike exciton blueshift. The phase space in a partially filled LL will also facilitate the carrier scattering and hence broaden the exciton peak and reduce the peak conductivity value. Based on this analysis, we use the exciton width maxima and conductivity minima to identify the V_g positions of half-filled LLs [Figs. 2(c)–2(d)].

The above qualitative picture can be quantified by semiempirical calculations. We have calculated the exciton conductivity spectrum by solving the massive Dirac equation for the electron and hole, including their screened Coulomb interaction, for monolayer WSe_2 under magnetic field (see Supplemental Material [47]). We only consider the hole filling in the K valley. Our calculations reproduce the main observation and confirm the assignment of half-filled LL positions [Figs. 2(e)–2(h)].

We next discuss the reflection results on the electron side. The electrons are injected into the K' valley, which lies below the K valley, in the conduction band under the magnetic field [Fig. 1] [15]. The K'-valley electrons have no state-filling effect on the K-valley excitons, though they can screen the excitonic interaction. In our results, the K-valley A^0 exciton shows no oscillation on the electron side [Fig. 2(d)]. This indicates weak influence of the K'-valley LL filling on the K-valley excitons.

The LL filling in the K' conduction valley, however, is found to induce noticeable quantum oscillations in the A^- intervalley trion, which couples a K-valley exciton and the K'-valley Fermi sea. The A^- trion exhibits two kinks in the conductivity and resonance energy when V_g increases [Fig. 4]. We assign these kinks as the half-filled LL positions. When the Fermi energy lies within a LL, the phase space and free carriers in the partially filled LL can facilitate the trion formation, enhance the trion oscillator strength, and renormalize the trion energy. When the Fermi energy lies within a LL gap, the suppression of carrier scattering can hinder the trion formation.

Our observed exciton and trion oscillations allow us to identify the V_g positions of half-filled LLs in the K valence valley and lower K' conduction valley, respectively. Figure 2(e) displays these LL V_g positions as a function of magnetic field (see Supplemental Material for data at other magnetic fields [47]). By calculating the Landau fan diagram, we fit the data on both the electron and hole sides by using a BN dielectric constant 3.06 [79] and the LL density of states with no spin and valley degeneracy [lines in Fig. 2(e)]. Comparison with theory confirms our observation of valence LLs with filling factors $n = -0$ to -6 and conduction LLs with $n = +0, +1$; all the observed LLs are spin and valley polarized. Notably, we directly resolve the two $n = 0$ LLs in the lower K'-valley conduction band and

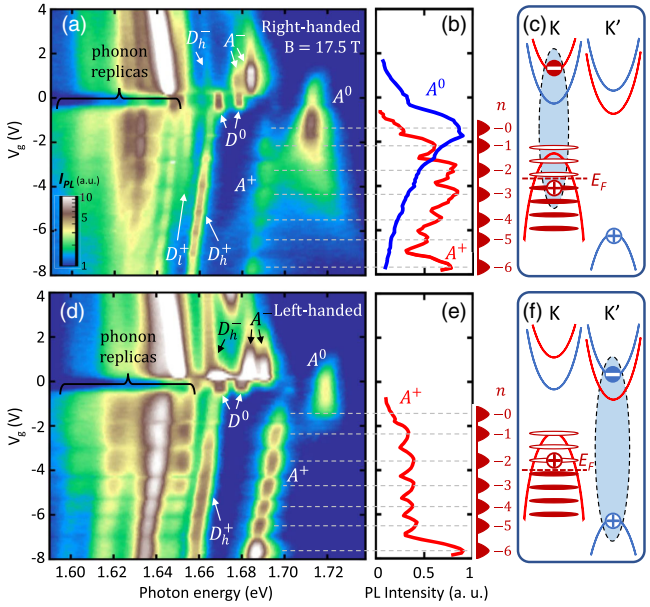

FIG. 5. (a) The gate-dependent photoluminescence (PL) map at right-handed circular polarization, which reveals the K-valley emission of bright excitonic states (A), under 532-nm continuous laser excitation at $B = 17.5$ T and $T \sim 4$ k. (b) The normalized integrated PL intensity for the A^0 exciton (blue) and A^+ trion (red) in (a). The dashed lines denote the estimated half-filled LL positions. (c) The schematic band configuration of K valley A^+ trion with the relevant LLs and Fermi energy (E_F) under the magnetic field. The K'-valley hole comes from the laser excitation. (d)–(f) Similar figures as (a)–(c) for left-handed circular polarization, which reveals the K'-valley emission of bright excitonic states. In (a) and (d), which share the same color scale, we also observe the emission of dark excitonic states (D) from both valleys due to their linear polarization as well as a series of phonon replicas of the dark states.

top K-valley valence band [Fig. 1]. These two LLs are induced by the Berry curvature of massive Dirac fermions [22–24]. Our results complement prior research that probed the $|n| \geq 0$ LLs in the upper conduction band and top valence band through inter-LL optical transitions [38].

Our discussion above is limited to absorption properties. We have also observed quantum oscillations in the excitonic photoluminescence (PL) [Fig. 5]. Figure 5(a) displays the right-handed PL map at $B = 17.5$ T, which reveals the K-valley emission of the bright exciton (A^0) and trions (A^-, A^+). The A^+ trions emit weak but observable PL [Fig. 5(a)], unlike the complete A^+ suppression in absorption [Fig. 2(d)]. This is because the laser excitation can generate transient holes in the K' valley to form intervalley trions [Fig. 5(c)]. We observe oscillations in the PL intensity of both the A^0 exciton and A^+ trion from the K valley, but their oscillations are out of phase to each other [Fig. 5(b)]. The PL intensity of excitons and trions reflects their steady-state population in monolayer WSe_2. According to the exciton line width in Fig. 3(c), the exciton lifetime is significantly shortened at half LL filling due to the enhanced carrier scattering. This implies a higher exciton-to-trion relaxation rate at half LL filling. Moreover, the phase space in a partially filled LL favors trion formation. We thus expect the exciton population to drop and the trion population to increase at half LL filling. This picture qualitatively explains the opposite oscillations of A^0 and A^+ PL intensity in our experiment. The A^+ PL maxima should correspond to the half-filled LL positions [Figs. 5(a)–5(b)].

Figure 5(d) displays the left-handed PL map at $B = 17.5$ T, which reveals the emission of bright excitons and trions from the K' valley [Fig. 5(f)]. On the hole side, the A^0 exciton is quenched and the A^+ trion dominates, because the injected holes in the K valley can efficiently couple to the K'-valley exciton to form intervalley trions [Fig. 5(f)]. The A^+ PL intensity oscillates as the hole density increases [Fig. 5(e)]. The A^+ PL maxima should correspond to partially filled LLs, whose free carriers and phase space favor the trion formation, like the A^- oscillation in Fig. 4. Our experiment could not resolve any appreciable oscillation of A^+ PL energy and peak width.

Remarkably, our PL maps also reveal quantum oscillations of dark trions (D^+) and their phonon replicas on the hole side [Figs. 5(a) and 5(d)]. As the dark exciton (D^0) and trions (D^+, D^-) in monolayer WSe_2 emit linearly polarized light, our circularly polarized PL maps show their emission from both valleys, which is split into two lines under magnetic field [45]. The lower-energy line (D_l^+) and all replicas on the hole side oscillate in phase with A^+ (Fig. 5; Fig. S14 [47]). This is reasonable because partially filled LLs also favor the dark-trion formation, and the dark-trion replicas acquire oscillator strength from the A^+ state through trion-phonon interaction [46,53]. But surprisingly, the higher-energy line (D_h^+) oscillates oppositely with A^+ and D_l^+ (Fig. S14 [47]). We speculate that this is because the D_l^+ and D_h^+ states compete for the insufficient transient holes in the K' valley to form trions. When one prevails, the other is suppressed, thus leading to opposite oscillations between them (see more discussion in the Supplemental Material [47]).

Our observation of numerous valley-polarized LLs reveals extraordinarily large valley Zeeman shift beyond a single-particle picture. Our reflectance contrast maps show seven LLs ($n = -0$ to -6) before the exciton is suppressed [Figs. 2(c) and 2(d)]. Our PL maps also show seven LLs ($n = -0$ to -6) before the A^+ PL is abruptly intensified and the A^+ oscillation is smoothened (Figs. S9 and S11 in the Supplemental Material [47]). Both indicate that the injected holes start to occupy the K' valley after the K valley. The energy mixing of two valleys can facilitate the carrier scattering, enhance the trion formation, and obscure the trion oscillation. Therefore, the K valence valley should be at least 6 LL spacings higher than the K' valence valley. The LL energy spacing is $2\mu_B B m_0/m^*$, where μ_B is the Bohr magneton, m_0 is the free electron

mass, and $m^* \approx 0.4\ m_0$ is the hole effective mass in monolayer WSe_2 [57]. The K valley is thus at least 30 $\mu_B B$ above the K' valley. The g factor of the K valence valley is deduced to be ~15. This far exceeds the g factor (5.5) predicted in a single-particle model [15,47]. This deviation implies strong many-body interactions in the system.

Similar interaction-driven enhancement of the g factor is found in the conduction valleys. After filling the $n = +0$, $+1$ LLs in the K' valley, the A^- feature is noticeably broadened and the quantum oscillation disappears [Fig. 4]. This signifies that the injected electrons start to occupy the K valley after the K' valley. The mixing of intra- and inter-valley trions broaden and smoothen the A^- feature (Fig. S7 [47]). We therefore deduce that the K conduction valley is at least 1 LL spacing higher than the K' conduction valley. Given the electron effective mass $m^* \approx 0.4 m_0$ [30,57,58], the K valley is at least 5 $\mu_B B$ above the K' valley. The g factor of the K-conduction valley is thus at least 2.5. This exceeds the g factor (1.5) predicted by a single-particle model. Recent experiments also reported the g-factor enhancement in the conduction valleys of bilayer MoS_2 [37], monolayer and bilayer $MoSe_2$ [34,80], and the valence valleys of monolayer WSe_2 [39,81]. Here we further demonstrate that many-body interactions can enhance the g factors in both the conduction and valence valleys of gated monolayer WSe_2 [Figs. 1(a) and 1(b)].

In summary, we have observed quantum oscillations in the absorption and luminescence of exciton and trion states in monolayer WSe_2 under magnetic field. The plateaus in the exciton energy shift indicate well-separated LLs. The enhanced g factors imply strong many-body interactions. The combined observation of the lowest LLs and strong many-body interactions suggest that fractional quantum Hall states can emerge in monolayer WSe_2. In addition, the $n = 0$ half-filled LLs contain a very low density ($\sim 1.4 \times 10^{11}$ cm^{-2}) of free carriers (not trapped by defects). This density corresponds to a large Wigner-Seitz radius $r_s \approx 25$ [47], close to the predicted condition $r_s \gtrsim 31$ of Wigner crystallization in two dimensions [62]. Therefore, our optical methods, inert to the contact resistance, may help probe the fractional quantum Hall states and Wigner crystals in monolayer valley semiconductors.

We thank Dmitry Smirnov and Zhengguang Lu for assistance in the experiments. A portion of this work was performed at the National High Magnetic Field Laboratory, which is supported by the National Science Foundation Cooperative Agreement No. DMR-1644779 and the State of Florida. Y.-C. C. is supported by Ministry of Science and Technology (Taiwan) under Grants No. MOST 107-2112-M-001-032 and No. MOST 108-2112-M-001-041. K. W. and T. T. acknowledge support from the Elemental Strategy Initiative conducted by the MEXT, Japan and the CREST (JPMJCR15F3), JST.

E. L. and J. v. B. contributed equally to this work.

*Corresponding author.
joshua.lui@ucr.edu

[1] K. F. Mak, C. Lee, J. Hone, J. Shan, and T. F. Heinz, Atomically Thin MoS_2: A New Direct-Gap Semiconductor, Phys. Rev. Lett. **105**, 136805 (2010).
[2] A. Splendiani, L. Sun, Y. Zhang, T. Li, J. Kim, C.-Y. Chim, G. Galli, and F. Wang, Emerging photoluminescence in monolayer MoS_2, Nano Lett. **10**, 1271 (2010).
[3] G. Wang, A. Chernikov, M. M. Glazov, T. F. Heinz, X. Marie, T. Amand, and B. Urbaszek, Colloquium: Excitons in atomically thin transition metal dichalcogenides, Rev. Mod. Phys. **90**, 021001 (2018).
[4] D. Xiao, G.-B. Liu, W. Feng, X. Xu, and W. Yao, Coupled Spin and Valley Physics in Monolayers of MoS_2 and other Group-VI Dichalcogenides, Phys. Rev. Lett. **108**, 196802 (2012).
[5] G.-B. Liu, W.-Y. Shan, Y. Yao, W. Yao, and D. Xiao, Three-band tight-binding model for monolayers of group-VIB transition metal dichalcogenides, Phys. Rev. B **88**, 085433 (2013).
[6] K. Kośmider, J. W. González, and J. Fernández-Rossier, Large spin splitting in the conduction band of transition metal dichalcogenide monolayers, Phys. Rev. B **88**, 245436 (2013).
[7] X. Xu, W. Yao, D. Xiao, and T. F. Heinz, Spin and pseudospins in layered transition metal dichalcogenides, Nat. Phys. **10**, 343 (2014).
[8] A. Chernikov, T. C. Berkelbach, H. M. Hill, A. Rigosi, Y. Li, O. B. Aslan, D. R. Reichman, M. S. Hybertsen, and T. F. Heinz, Exciton Binding Energy and Nonhydrogenic Rydberg Series in Monolayer WS_2, Phys. Rev. Lett. **113**, 076802 (2014).
[9] K. He, N. Kumar, L. Zhao, Z. Wang, K. F. Mak, H. Zhao, and J. Shan, Tightly Bound Excitons in Monolayer WSe_2, Phys. Rev. Lett. **113**, 026803 (2014).
[10] A. V. Stier, N. P. Wilson, K. A. Velizhanin, J. Kono, X. Xu, and S. A. Crooker, Magnetooptics of Exciton Rydberg States in a Monolayer Semiconductor, Phys. Rev. Lett. **120**, 057405 (2018).
[11] J. A. Schuller, S. Karaveli, T. Schiros, K. He, S. Yang, I. Kymissis, J. Shan, and R. Zia, Orientation of luminescent excitons in layered nanomaterials, Nat. Nanotechnol. **8**, 271 (2013).
[12] T. Cao, G. Wang, W. Han, H. Ye, C. Zhu, J. Shi, Q. Niu, P. Tan, E. Wang, B. Liu, and J. Feng, Valley-selective circular dichroism of monolayer molybdenum disulphide, Nat. Commun. **3**, 887 (2012).
[13] K. F. Mak, K. He, J. Shan, and T. F. Heinz, Control of valley polarization in monolayer MoS_2 by optical helicity, Nat. Nanotechnol. **7**, 494 (2012).
[14] H. Zeng, J. Dai, W. Yao, D. Xiao, and X. Cui, Valley polarization in MoS_2 monolayers by optical pumping, Nat. Nanotechnol. **7**, 490 (2012).
[15] G. Aivazian, Z. Gong, A. M. Jones, R.-L. Chu, J. Yan, D. G. Mandrus, C. Zhang, D. Cobden, W. Yao, and X. Xu, Magnetic control of valley pseudospin in monolayer WSe_2, Nat. Phys. **11**, 148 (2015).
[16] Y. Li, J. Ludwig, T. Low, A. Chernikov, X. Cui, G. Arefe, Y. D. Kim, A. M. van der Zande, A. Rigosi, H. M. Hill, S. H. Kim, J. Hone, Z. Li, D. Smirnov, and T. F. Heinz, Valley

Splitting and Polarization by the Zeeman Effect in Monolayer $MoSe_2$, Phys. Rev. Lett. **113**, 266804 (2014).
[17] D. MacNeill, C. Heikes, K. F. Mak, Z. Anderson, A. Kormányos, V. Zólyomi, J. Park, and D. C. Ralph, Breaking of Valley Degeneracy by Magnetic Field in Monolayer $MoSe_2$, Phys. Rev. Lett. **114**, 037401 (2015).
[18] A. Srivastava, M. Sidler, A. V. Allain, D. S. Lembke, A. Kis, and A. Imamoğlu, Valley Zeeman effect in elementary optical excitations of monolayer WSe_2, Nat. Phys. **11**, 141 (2015).
[19] G. Wang, L. Bouet, M. M. Glazov, T. Amand, E. L. Ivchenko, E. Palleau, X. Marie, and B. Urbaszek, Magneto-optics in transition metal diselenide monolayers, 2D Mater. **2**, 034002 (2015).
[20] J. Have, G. Catarina, T. G. Pedersen, and N. M. R. Peres, Monolayer transition metal dichalcogenides in strong magnetic fields: Validating the Wannier model using a microscopic calculation, Phys. Rev. B **99**, 035416 (2019).
[21] D. K. Efimkin and A. H. MacDonald, Exciton-polarons in doped semiconductors in a strong magnetic field, Phys. Rev. B **97**, 235432 (2018).
[22] A. Kormányos, P. Rakyta, and G. Burkard, Landau levels and Shubnikov–de Haas oscillations in monolayer transition metal dichalcogenide semiconductors, New J. Phys. **17**, 103006 (2015).
[23] T. Cai, S. A. Yang, X. Li, F. Zhang, J. Shi, W. Yao, and Q. Niu, Magnetic control of the valley degree of freedom of massive Dirac fermions with application to transition metal dichalcogenides, Phys. Rev. B **88**, 115140 (2013).
[24] F. Rose, M. O. Goerbig, and F. Piéchon, Spin- and valley-dependent magneto-optical properties of MoS_2, Phys. Rev. B **88**, 125438 (2013).
[25] X. Du, I. Skachko, F. Duerr, A. Luican, and E. Y. Andrei, Fractional quantum Hall effect and insulating phase of dirac electrons in graphene, Nature (London) **462**, 192 (2009).
[26] K. I. Bolotin, F. Ghahari, M. D. Shulman, H. L. Stormer, and P. Kim, Observation of the fractional quantum Hall effect in graphene, Nature (London) **462**, 196 (2009).
[27] E. Y. Andrei, G. Deville, D. C. Glattli, F. I. B. Williams, E. Paris, and B. Etienne, Observation of a Magnetically Induced Wigner Solid, Phys. Rev. Lett. **60**, 2765 (1988).
[28] V. J. Goldman, M. Santos, M. Shayegan, and J. E. Cunningham, Evidence for Two-Dimensional Quantum Wigner Crystal, Phys. Rev. Lett. **65**, 2189 (1990).
[29] X. Cui, G.-H. Lee, Y. D. Kim, G. Arefe, P. Y. Huang, C.-H. Lee, D. A. Chenet, X. Zhang, L. Wang, F. Ye, F. Pizzocchero, B. S. Jessen, K. Watanabe, T. Taniguchi, D. A. Muller, T. Low, P. Kim, and J. Hone, Multi-terminal transport measurements of MoS_2 using a van der Waals heterostructure device platform, Nat. Nanotechnol. **10**, 534 (2015).
[30] S. Xu, Z. Wu, H. Lu, Y. Han, G. Long, X. Chen, T. Han, W. Ye, Y. Wu, J. Lin, J. Shen, Y. Cai, Y. He, F. Zhang, R. Lortz, C. Cheng, and N. Wang, Universal low-temperature Ohmic contacts for quantum transport in transition metal dichalcogenides, 2D Mater. **3**, 021007 (2016).
[31] Z. Wu, S. Xu, H. Lu, A. Khamoshi, G.-B. Liu, T. Han, Y. Wu, J. Lin, G. Long, Y. He, Y. Cai, Y. Yao, F. Zhang, and N. Wang, Even–odd layer-dependent magnetotransport of high-mobility Q-valley electrons in transition metal disulfides, Nat. Commun. **7**, 12955 (2016).
[32] B. Fallahazad, H. C. P. Movva, K. Kim, S. Larentis, T. Taniguchi, K. Watanabe, S. K. Banerjee, and E. Tutuc, Shubnikov-de Haas Oscillations of High-Mobility Holes in Monolayer and Bilayer WSe_2: Landau Level Degeneracy, Effective Mass, and Negative Compressibility, Phys. Rev. Lett. **116**, 086601 (2016).
[33] R. Pisoni, Y. Lee, H. Overweg, M. Eich, P. Simonet, K. Watanabe, T. Taniguchi, R. Gorbachev, T. Ihn, and K. Ensslin, Gate-defined one-dimensional channel and broken symmetry states in MoS_2 van der Waals heterostructures, Nano Lett. **17**, 5008 (2017).
[34] S. Larentis, H. C. P. Movva, B. Fallahazad, K. Kim, A. Behroozi, T. Taniguchi, K. Watanabe, S. K. Banerjee, and E. Tutuc, Large effective mass and interaction-enhanced Zeeman splitting of K-valley electrons in $MoSe_2$, Phys. Rev. B **97**, 201407(R) (2018).
[35] R. Pisoni, A. Kormányos, M. Brooks, Z. Lei, P. Back, M. Eich, H. Overweg, Y. Lee, P. Rickhaus, K. Watanabe, T. Taniguchi, A. Imamoglu, G. Burkard, T. Ihn, and K. Ensslin, Interactions and Magnetotransport through Spin-Valley Coupled Landau Levels in Monolayer MoS_2, Phys. Rev. Lett. **121**, 247701 (2018).
[36] H. C. P. Movva, T. Lovorn, B. Fallahazad, S. Larentis, K. Kim, T. Taniguchi, K. Watanabe, S. K. Banerjee, A. H. MacDonald, and E. Tutuc, Tunable Γ-K Valley Populations in Hole-Doped Trilayer WSe_2, Phys. Rev. Lett. **120**, 107703 (2018).
[37] J. Lin, T. Han, B. A. Piot, Z. Wu, S. Xu, G. Long, L. An, P. Cheung, P.-P. Zheng, P. Plochocka, X. Dai, D. K. Maude, F. Zhang, and N. Wang, Determining interaction enhanced valley susceptibility in spin-valley-locked MoS_2, Nano Lett. **19**, 1736 (2019).
[38] Z. Wang, J. Shan, and K. F. Mak, Valley- and spin-polarized Landau levels in monolayer WSe_2, Nat. Nanotechnol. **12**, 144 (2017).
[39] M. V. Gustafsson, M. Yankowitz, C. Forsythe, D. Rhodes, K. Watanabe, T. Taniguchi, J. Hone, X. Zhu, and C. R. Dean, Ambipolar Landau levels and strong band-selective carrier interactions in monolayer WSe_2, Nat. Mater. **17**, 411 (2018).
[40] T. Smoleński, O. Cotlet, A. Popert, P. Back, Y. Shimazaki, P. Knüppel, N. Dietler, T. Taniguchi, K. Watanabe, M. Kroner, and A. Imamoglu, Interaction-Induced Shubnikov-de Haas Oscillations in Optical Conductivity of Monolayer $MoSe_2$, Phys. Rev. Lett. **123**, 097403 (2019).
[41] M. Sidler, P. Back, O. Cotlet, A. Srivastava, T. Fink, M. Kroner, E. Demler, and A. Imamoglu, Fermi polaron-polaritons in charge-tunable atomically thin semiconductors, Nat. Phys. **13**, 255 (2017).
[42] D. K. Efimkin and A. H. MacDonald, Many-body theory of trion absorption features in two-dimensional semiconductors, Phys. Rev. B **95**, 035417 (2017).
[43] Y.-C. Chang, S.-Y. Shiau, and M. Combescot, Crossover from trion-hole complex to exciton-polaron in n-doped two-dimensional semiconductor quantum wells, Phys. Rev. B **98**, 235203 (2018).
[44] E. Liu, J. van Baren, T. Taniguchi, K. Watanabe, Y.-C. Chang, and C. H. Lui, Magnetophotoluminescence of

exciton Rydberg states in monolayer WSe_2, Phys. Rev. B **99**, 205420 (2019).
[45] E. Liu, J. van Baren, Z. Lu, M. M. Altaiary, T. Taniguchi, K. Watanabe, D. Smirnov, and C. H. Lui, Gate Tunable Dark Trions in Monolayer WSe_2, Phys. Rev. Lett. **123**, 027401 (2019).
[46] E. Liu, J. van Baren, Z. Lu, T. Taniguchi, K. Watanabe, D. Smirnov, Y.-C. Chang, and C. H. Lui, Valley-selective chiral phonon replicas of dark excitons and trions in monolayer WSe_2, Phys. Rev. Research **1**, 032007(R) (2019).
[47] See Supplemental Material at http://link.aps.org/supplemental/10.1103/PhysRevLett.124.097401, which includes detailed description of experiments, additional data, calculations, and Refs. [8,15–18,23,30,34,37,39, 42–46,48–76].
[48] E. Hecht, *Optics* 3rd ed. (Addison-Wesley, New York, 1998).
[49] J. W. Weber, V. E. Calado, and M. C. M. v. d. Sanden, Optical constants of graphene measured by spectroscopic ellipsometry, Appl. Phys. Lett. **97**, 091904 (2010).
[50] A. Segura, L. Artús, R. Cuscó, T. Taniguchi, G. Cassabois, and B. Gil, Natural optical anisotropy of h-BN: Highest giant birefringence in a bulk crystal through the mid-infrared to ultraviolet range, Phys. Rev. Mater. **2**, 024001 (2018).
[51] S.-Y. Lee, T.-Y. Jeong, S. Jung, and K.-J. Yee, Refractive index dispersion of hexagonal boron nitride in the visible and near-infrared, Phys. Status Solidi (b) **256**, 1800417 (2019).
[52] A. B. Kuzmenko, Kramers–Kronig constrained variational analysis of optical spectra, Rev. Sci. Instrum. **76**, 083108 (2005).
[53] Z. Li, T. Wang, C. Jin, Z. Lu, Z. Lian, Y. Meng, M. Blei, S. Gao, T. Taniguchi, K. Watanabe, T. Ren, S. Tongay, L. Yang, D. Smirnov, T. Cao, and S.-F. Shi, Emerging photoluminescence from the dark-exciton phonon replica in monolayer WSe_2, Nat. Commun. **10**, 2469 (2019).
[54] C. R. Dean, A. F. Young, I. Meric, C. Lee, L. Wang, S. Sorgenfrei, K. Watanabe, T. Taniguchi, P. Kim, K. L. Shepard, and J. Hone, Boron nitride substrates for high-quality graphene electronics, Nat. Nanotechnol. **5**, 722 (2010).
[55] A. Laturia, M. L. Van de Put, and W. G. Vandenberghe, Dielectric properties of hexagonal boron nitride and transition metal dichalcogenides: from monolayer to bulk, npj 2D Mater. Appl. **2**, 6 (2018).
[56] J. R. Schaibley, H. Yu, G. Clark, P. Rivera, J. S. Ross, K. L. Seyler, W. Yao, and X. Xu, Valleytronics in 2D materials, Nat. Rev. Mater. **1**, 16055 (2016).
[57] P. V. Nguyen, N. C. Teutsch, N. P. Wilson, J. Kahn, X. Xia, A. J. Graham, V. Kandyba, A. Giampietri, A. Barinov, G. C. Constantinescu, N. Yeung, N. D. M. Hine, X. Xu, D. H. Cobden, and N. R. Wilson, Visualizing electrostatic gating effects in two-dimensional heterostructures, Nature (London) **572**, 220 (2019).
[58] K. Andor, B. Guido, G. Martin, F. Jaroslav, Z. Viktor, D. D. Neil, and F. k. Vladimir, $k\ldots p$ theory for two-dimensional transition metal dichalcogenide semiconductors, 2D Mater. **2**, 022001 (2015).
[59] K. F. Mak, K. He, C. Lee, G. H. Lee, J. Hone, T. F. Heinz, and J. Shan, Tightly bound trions in monolayer MoS_2, Nat. Mater. **12**, 207 (2013).
[60] B. Tanatar and D. M. Ceperley, Ground state of the two-dimensional electron gas, Phys. Rev. B **39**, 5005 (1989).
[61] C. Attaccalite, S. Moroni, P. Gori-Giorgi, and G. B. Bachelet, Correlation Energy and Spin Polarization in the 2D Electron Gas, Phys. Rev. Lett. **88**, 256601 (2002).
[62] N. D. Drummond and R. J. Needs, Phase Diagram of the Low-Density Two-Dimensional Homogeneous Electron Gas, Phys. Rev. Lett. **102**, 126402 (2009).
[63] M. Zarenia, D. Neilson, B. Partoens, and F. M. Peeters, Wigner crystallization in transition metal dichalcogenides: A new approach to correlation energy, Phys. Rev. B **95**, 115438 (2017).
[64] I. Filikhin, R. Y. Kezerashvili, S. M. Tsiklauri, and B. Vlahovic, Trions in bulk and monolayer materials: Faddeev equations and hyperspherical harmonics, Nanotechnology **29**, 124002 (2018).
[65] A. Ramasubramaniam, Large excitonic effects in monolayers of molybdenum and tungsten dichalcogenides, Phys. Rev. B **86**, 115409 (2012).
[66] H. Shi, H. Pan, Y.-W. Zhang, and B. I. Yakobson, Quasiparticle band structures and optical properties of strained monolayer MoS_2 and WS_2, Phys. Rev. B **87**, 155304 (2013).
[67] W. Cai and C. S. Ting, Screening effect on the Landau-level broadening for electrons in GaAs-$Ga_{1-x}Al_xAs$ heterojunctions, Phys. Rev. B **33**, 3967 (1986).
[68] S. Schmitt-Rink, D. S. Chemla, and D. A. B. Miller, Linear and nonlinear optical properties of semiconductor quantum wells, Adv. Phys. **38**, 89 (1989).
[69] N. S. Rytova, Screened potential of a point charge in a thin film, arXiv:1806.00976.
[70] L. Keldysh, Coulomb interaction in thin semiconductor and semimetal films, JETP Lett. **29**, 658 (1979).
[71] G. Sanders and Y.-C. Chang, Theory of photoabsorption in modulation-doped semiconductor quantum wells, Phys. Rev. B **35**, 1300 (1987).
[72] R. Y. Kezerashvili and S. M. Tsiklauri, Trion and biexciton in monolayer transition metal dichalcogenides, Few-Body Syst. **58**, 18 (2017).
[73] E. Courtade, M. Semina, M. Manca, M. M. Glazov, C. Robert, F. Cadiz, G. Wang, T. Taniguchi, K. Watanabe, M. Pierre, W. Escoffier, E. L. Ivchenko, P. Renucci, X. Marie, T. Amand, and B. Urbaszek, Charged excitons in monolayer WSe_2: Experiment and theory, Phys. Rev. B **96**, 085302 (2017).
[74] K. S. Thygesen, Calculating excitons, plasmons, and quasiparticles in 2D materials and van der Waals heterostructures, 2D Mater. **4**, 022004 (2017).
[75] F. Stern, Polarizability of a Two-Dimensional Electron Gas, Phys. Rev. Lett. **18**, 546 (1967).
[76] H. Chu and Y.-C. Chang, Line-shape theory of magneto-absorption in semiconductor superlattices, Phys. Rev. B **40**, 5497 (1989).
[77] A. Chernikov, A. M. Van Der Zande, H. M. Hill, A. F. Rigosi, A. Velauthapillai, J. Hone, and T. F. Heinz, Electrical Tuning of Exciton Binding Energies in Monolayer WS_2, Phys. Rev. Lett. **115**, 126802 (2015).

[78] S.-Y. Shiau, M. Combescot, and Y.-C. Chang, Trion ground state, excited states, and absorption spectrum using electron-exciton basis, Phys. Rev. B **86**, 115210 (2012).

[79] M. Yankowitz, J. Jung, E. Laksono, N. Leconte, B. L. Chittari, K. Watanabe, T. Taniguchi, S. Adam, D. Graf, and C. R. Dean, Dynamic band-structure tuning of graphene moiré superlattices with pressure, Nature (London) **557**, 404 (2018).

[80] P. Back, M. Sidler, O. Cotlet, A. Srivastava, N. Takemura, M. Kroner, and A. Imamoğlu, Giant Paramagnetism-Induced Valley Polarization of Electrons in Charge-Tunable Monolayer $MoSe_2$, Phys. Rev. Lett. **118**, 237404 (2017).

[81] Z. Wang, K. F. Mak, and J. Shan, Strongly Interaction-Enhanced Valley Magnetic Response in Monolayer WSe_2, Phys. Rev. Lett. **120**, 066402 (2018).